ELECTRONIC SUPPLEMENTARY INFORMATION (ESI)

Hydrogen Atom Transfer from 1,2- and 1,3-Diols to the Cumyloxyl Radical. The Role of Structural Effects on Metal-Ion Induced C–H Bond Deactivation

Teo Martin, Michela Salamone and Massimo Bietti *

Dipartimento di Scienze e Tecnologie Chimiche, Università "Tor Vergata", Via della Ricerca Scientifica, 1 I-00133 Rome, Italy.

1) Chart of the substrates **S2**

2) Experimental section **S3**

3) Laser flash photolysis studies: k_{obs} vs [substrate] plots **S4**

S3

4) References **S10**

1) Chart of the substrates

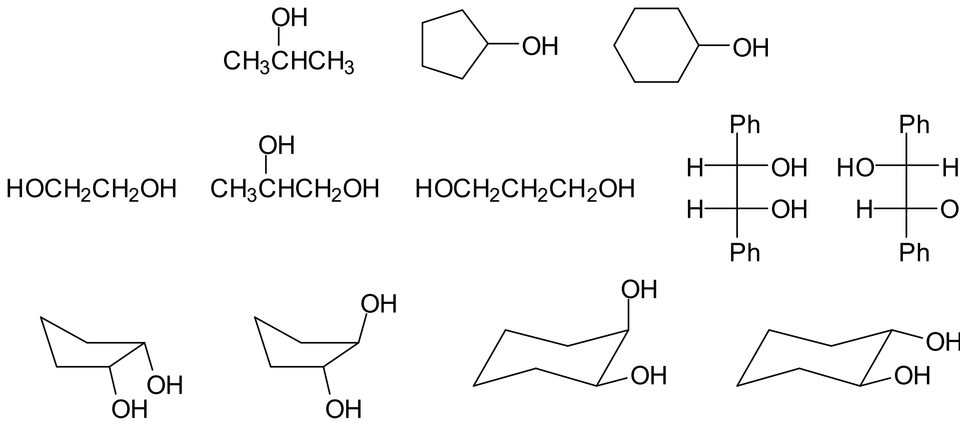

2) Experimental section

Materials. Spectroscopic grade acetonitrile was used in the kinetic experiments. Dicumyl peroxide, 2-propanol, 1,2-ethanediol, 1,2-propanediol (racemic), 1,3-propanediol, *meso*-1,2-diphenyl-1,2-ethanediol, *(1R,2R)*-1,2-diphenyl-1,2-ethanediol, cyclopentanol, cyclohexanol, *cis*-1,2-cyclopentanediol, *trans*-1,2-cyclopentanediol (racemic), *cis*-1,2-cyclohexanediol, *trans*-1,2-cyclohexanediol (racemic), were of the highest commercial quality available and were used as received. Lithium perchlorate ($LiClO_4$), magnesium perchlorate ($Mg(ClO_4)_2$), and calcium perchlorate ($Ca(ClO_4)_2$) were of the highest commercial quality available and were used as received without any drying procedure.

Laser flash photolysis studies. The time-resolved kinetic studies have been carried out by LFP employing a laser kinetic spectrometer using the third harmonic (355 nm) of a Q-switched Nd:YAG laser, delivering pulses of the duration of 8 ns. The laser energy has been adjusted by the use of the appropriate filter to ≤ 10 mJ/pulse. A 3.5 mL quartz cell (Suprasil, 10 mm × 10 mm) has been used and all the experiments have been carried out at T = 25±0.5 °C under magnetic stirring. Experiments have been typically carried out employing argon or nitrogen saturated acetonitrile solutions containing 1.0 M dicumyl peroxide. The observed rate constants (k_{obs}) have been obtained following the decay of the cumyloxyl radical ($CumO^•$) absorption band at 490 nm as a function of the concentration of added substrate. Second order rate constant (k_H) for the reactions of $CumO^•$ with the alcohol and diol substrates, in acetonitrile and in acetonitrile containing the metal ion salts, have been obtained from the slopes of the k_{obs} vs [substrate] plots at constant salt concentration (between 0.3 and 0.6 M). The concentration variation was performed by direct addition of the substrate to solutions containing dicumyl peroxide and the metal ion salt. The k_H values are the average at least two values obtained through independent experiments, with typical errors being ≤ 10 %. In all the graphs displayed in the following section (Figures S1-S11), the different intercepts of the plots reflect the effect of the metal ion on the CumO• β-scission.[S1]

The upper limit to k_H, estimated for the reactions of CumO• with 1,2- and 1,3-diol substrates carried out in the presence of $Ca(ClO_4)_2$ (Table 1), is derived from the comparison of the kinetic effects observed in these reactions, with those observed previously in the corresponding reactions of CumO• with *N*,*N*-dimethylformamide and *N*,*N*-dimethylacetamide where, for both substrates, strong deactivation toward HAT was observed in the presence of $Ca(ClO_4)_2$, up to $[substrate]/[Ca(ClO_4)_2] = 4$.[S1] Along this line, the comparable decrease in k_{obs} observed following substrate addition for 1,2-diols, 1,3-diols and tertiary alkanamides, points toward a negligible contribution of HAT to k_{obs}, leading, by comparison with the results obtained in the presence of $LiClO_4$, to an upper limit to the rate constant for HAT from these substrates $k_H < 2 \times 10^4$ M^{-1} s^{-1}.

3) Laser flash photolysis studies: k_{obs} vs [substrate] plots

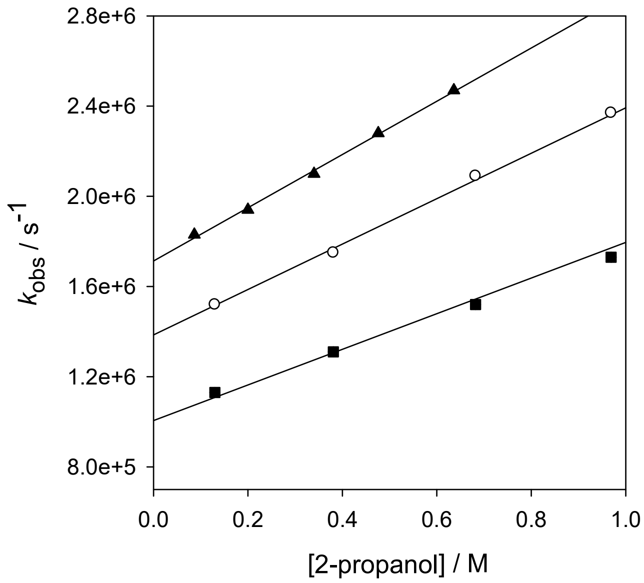

Figure S1. Plots of the observed rate constant (k_{obs}) against [2-propanol] for the reaction of CumO$^•$ generated by 355 nm LFP of an Ar-saturated MeCN solution containing 1.0 M dicumyl peroxide in the presence of a) 0.5 M $LiClO_4$ (white circles); b) 0.5 M $Mg(ClO_4)_2$ (black squares); c) 0.4 M $Ca(ClO_4)_2$ (black triangles) measured at T = 25 °C following the decay of CumO$^•$ at 490 nm. From the linear regression analysis: a) intercept = 1.39×10^6 s^{-1}, k_H = 1.01×10^6 M^{-1} s^{-1}, r^2 = 0.9990; b) intercept = 1.01×10^6 s^{-1}, k_H = 7.90×10^5 M^{-1} s^{-1}, r^2 = 0.9918; c) intercept = 1.71×10^6 s^{-1}, k_H = 1.18×10^6 M^{-1} s^{-1}, r^2 = 0.9978.

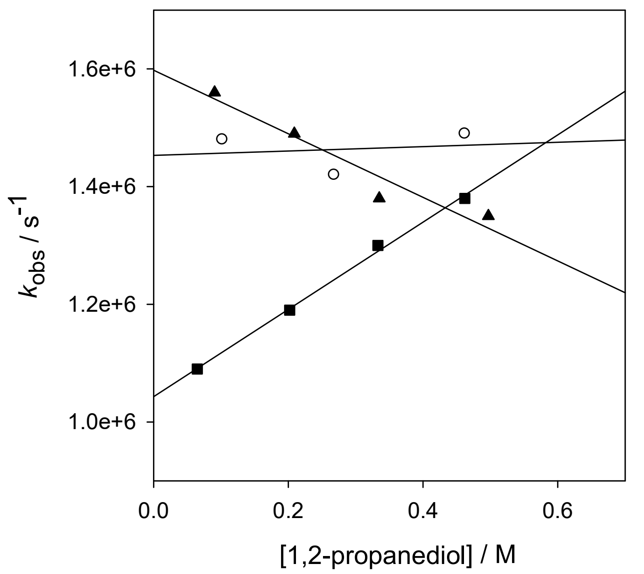

Figure S2. Plot of the observed rate constant (k_{obs}) against [1,2-propanediol] for the reaction of CumO$^•$ generated by 355 nm LFP of an Ar-saturated MeCN solution containing 1.0 M dicumyl peroxide in the presence of a) 0.5 M $LiClO_4$ (white circles); b) 0.5 M $Mg(ClO_4)_2$ (black squares); c) 0.4 M $Ca(ClO_4)_2$ (black triangles) measured at T = 25 °C following the decay of CumO$^•$ at 490 nm. From the linear regression analysis: a) intercept = 1.45×10^6 s^{-1}; b) intercept = 1.04×10^6 s^{-1}, k_H = 7.42×10^5 M^{-1} s^{-1}, r^2 = 0.9971; c) intercept = 1.59×10^6 s^{-1}.

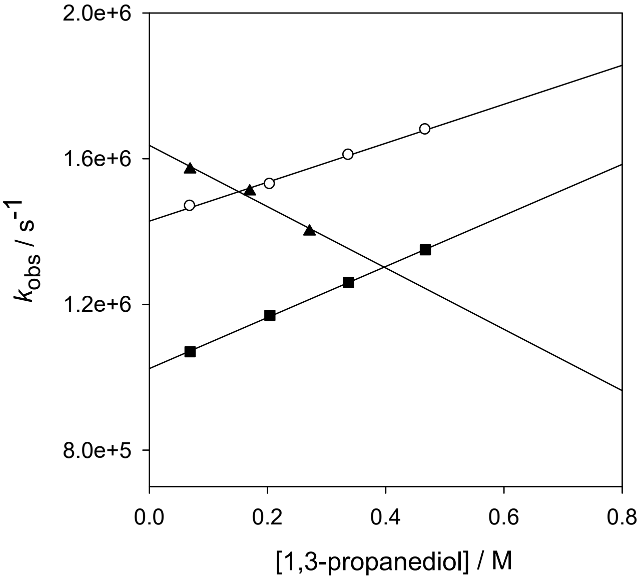

Figure S3. Plots of the observed rate constant (k_{obs}) against [1,3-propandiol] for the reaction of $CumO^{\bullet}$ generated by 355 nm LFP of an Ar-saturated MeCN solution containing 1.0 M dicumyl peroxide in the presence of a) $LiClO_4$ 0.5 M (white circles); b) $Mg(ClO_4)_2$ 0.5 M (black squares); c) $Ca(ClO_4)_2$ 0.39 M (black triangles), measured at T = 25 °C following the decay of $CumO^{\bullet}$ at 490 nm. From the linear regression analysis: a) intercept = 1.43×10^6 s^{-1}, k_H = 5.35×10^5 M^{-1} s^{-1}, r^2 = 0.9967; b) intercept = 1.02×10^6 s^{-1}, k_H = 7.02×10^5 M^{-1} s^{-1}, r^2 = 0.9906; c) intercept = 1.64×10^6 s^{-1}, r^2 = 0.9720.

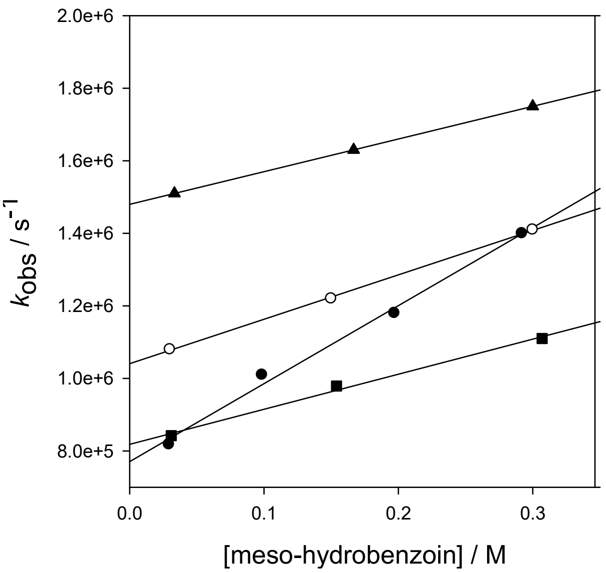

Figure S4. Plots of the observed rate constant (k_{obs}) against [meso-hydrobenzoin] for the reaction of $CumO^{\bullet}$ generated by 355 nm LFP of an Ar-saturated MeCN solution containing a) 1.0 M dicumyl peroxide (black circles); 1.0 M dicumyl peroxide in the presence of b) $LiClO_4$ 0.3 M (white circles); c) $Mg(ClO_4)_2$ 0.3 M (black squares); d) $Ca(ClO_4)_2$ 0.35 M (black triangles) measured at T = 25 °C following the decay of $CumO^{\bullet}$ at 490 nm. From the linear regression analysis: a) intercept = 7.71×10^5 s^{-1}, k_H = 2.15×10^6 M^{-1} s^{-1}, r^2 = 0.9935; b) intercept = 1.04×10^6 s^{-1}, k_H = 1.22×10^6 M^{-1} s^{-1}, r^2 = 0.9995; c) intercept = 8.19×10^5 s^{-1}, k_H = 9.66×10^5 M^{-1} s^{-1}, r^2 = 0.9999; intercept = 1.48×10^6 s^{-1}, k_H = 9.00×10^5 M^{-1} s^{-1}, r^2 = 0.9999.

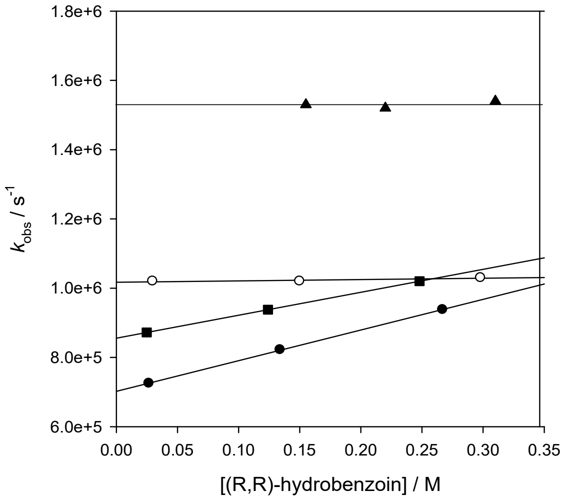

Figure S5. Plots of the observed rate constant (k_{obs}) against [(R,R)-hydrobenzoin] for the reaction of $CumO^{\bullet}$ generated by 355 nm LFP of an Ar-saturated MeCN solution containing a) 1.0 M dicumyl peroxide (black circles) and 1.0 M dicumyl peroxide in the presence of b) $LiClO_4$ 0.3 M (white circles); c) $Mg(ClO_4)_2$ 0.3 M (black squares); d) $Ca(ClO_4)_2$ 0.35 M (black triangles), measured at T = 25 °C following the decay of $CumO^{\bullet}$ at 490 nm. From the linear regression analysis: a) intercept = 7.02×10^5 s^{-1}, $k_H = 8.86 \times 10^5$ M^{-1} s^{-1}, $r^2 = 0.9999$; b) intercept = 1.02×10^6 s^{-1}, $k_H < 3 \times 10^4$ M^{-1} s^{-1}; c) intercept = 8.55×10^5 s^{-1}, $k_H = 6.63 \times 10^5$ M^{-1} s^{-1}, $r^2 = 0.9999$; d) intercept = 1.51×10^6 s^{-1}, $k_H < 3 \times 10^4$ M^{-1} s^{-1}.

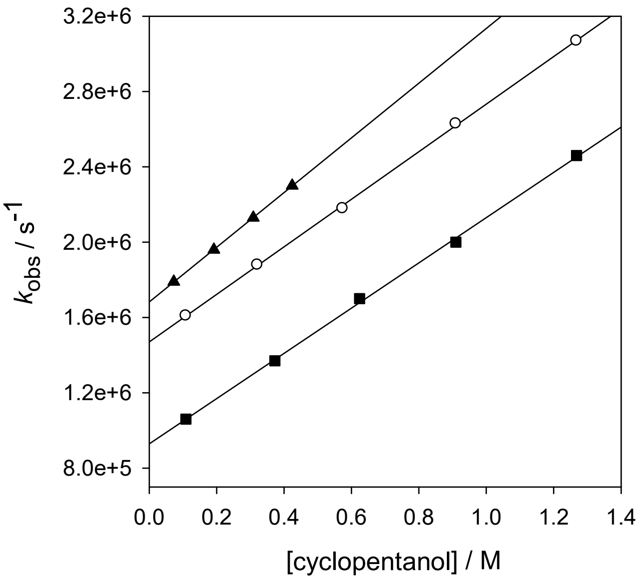

Figure S6. Plots of the observed rate constant (k_{obs}) against [cyclopentanol] for the reactions of $CumO^{\bullet}$ generated by 355 nm LFP of an Ar-saturated MeCN solution containing 1.0 M dicumyl peroxide in the presence of a) $LiClO_4$ 0.5 M (white circles); b) $Mg(ClO_4)_2$ 0.5 M (black squares); c) $Ca(ClO_4)_2$ 0.39 M (black triangles), measured at T = 25 °C following the decay of $CumO^{\bullet}$ at 490 nm. From the linear regression analysis: a) intercept = 1.47×10^6 s^{-1}, $k_H = 1.26 \times 10^6$ M^{-1} s^{-1}, $r^2 = 0.9997$; b) intercept = 9.28×10^5 s^{-1}, $k_H = 1.20 \times 10^6$ M^{-1} s^{-1}, $r^2 = 0.9991$; c) intercept = 1.68×10^6 s^{-1}, $k_H = 1.45 \times 10^6$ M^{-1} s^{-1}, $r^2 = 0.9999$.

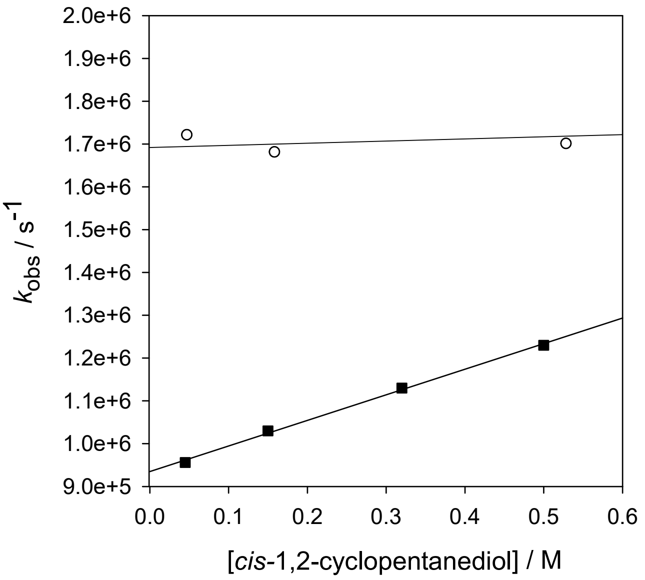

Figure S7. Plots of the observed rate constant (k_{obs}) against [*cis*-1,2-cyclopentandiol] for the reactions of CumO$^\bullet$ generated by 266 nm LFP Ar-saturated MeCN solution containing 1.0 M dicumyl peroxide in the presence of a) LiClO4 0.6M (white circles); (b) $Mg(ClO_4)_2$ 0.5 M (black squares) measured at T = 25 °C following the decay of CumO$^\bullet$ at 490 nm. From the linear regression analysis: a) intercept = 1.70×10^6 s^{-1}, $k_H < 2 \times 10^4$ M^{-1} s^{-1}; b) intercept = 9.35×10^5 s^{-1}, $k_H = 5.98 \times 10^5$ M^{-1} s^{-1}, $r^2 = 0.9978$.

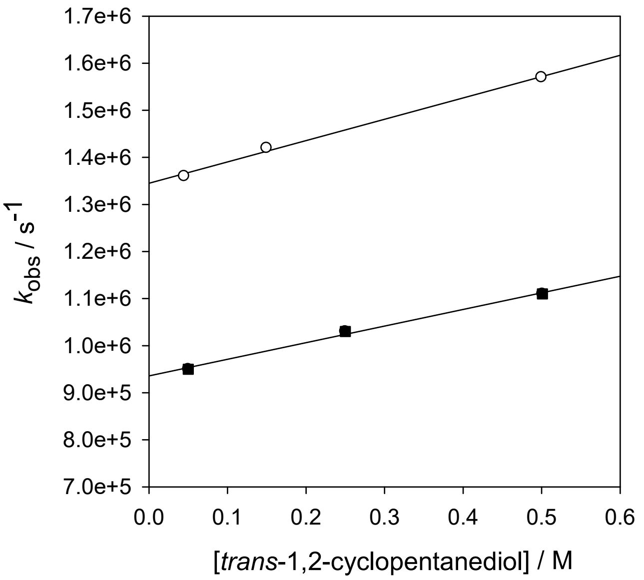

Figure S8. Plots of the observed rate constant (k_{obs}) against [*trans*-1,2-cyclopentanol] for the reactions of CumO$^\bullet$ generated by 355 nm LFP of an Ar-saturated MeCN solution containing 1.0 M dicumyl peroxide in the presence of a) $LiClO_4$ 0.5 M (white circles); b) $Mg(ClO_4)_2$ 0.5 M (black squares) measured at T = 25 °C following the decay of CumO$^\bullet$ at 490 nm. From the linear regression analysis: a) intercept = 1.35×10^6 s^{-1}, $k_H = 4.53 \times 10^5$ M^{-1} s^{-1}, $r^2 = 0.9965$; b) intercept = 9.36×10^5 s^{-1}, $k_H = 3.53 \times 10^5$ M^{-1} s^{-1}, $r^2 = 0.9958$.

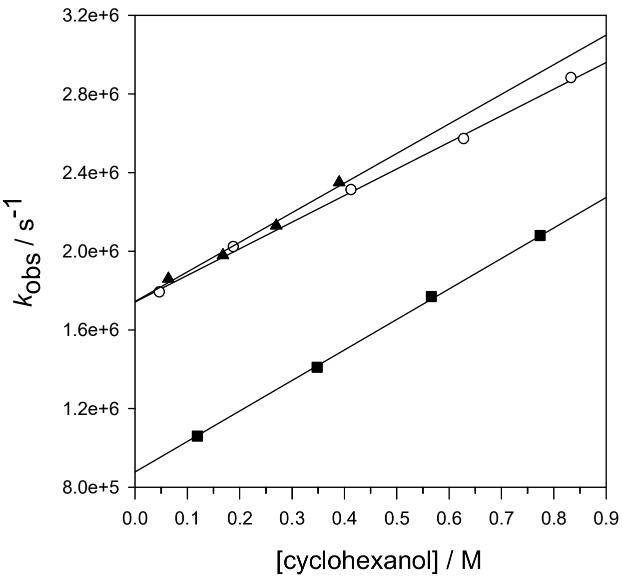

Figure S9. Plot of the observed rate constant (k_{obs}) against [cyclohexanol] for the reactions of CumO$^{\bullet}$ generated by 355 nm LFP of an Ar-saturated MeCN solution containing 1.0 M dicumyl peroxide in the presence of a) $LiClO_4$ 0.5 M (white circles); b) $Mg(ClO_4)_2$ 0.5 M (black squares); $Ca(ClO_4)_2$ 0.39 M (black triangles) measured at T = 25 °C following the decay of CumO$^{\bullet}$ at 490 nm. From the linear regression analysis: a) intercept = 1.74×10^6 s^{-1}, $k_H = 1.35 \times 10^6$ M^{-1} s^{-1}, r^2 = 0.9980; b) intercept = 8.77×10^5 s^{-1}, $k_H = 1.55 \times 10^6$ M^{-1} s^{-1}, r^2 = 0.9997; c) intercept = 1.74×10^6 s^{-1}, $k_H = 1.51 \times 10^6$ M^{-1} s^{-1}, r^2 = 0.9892.

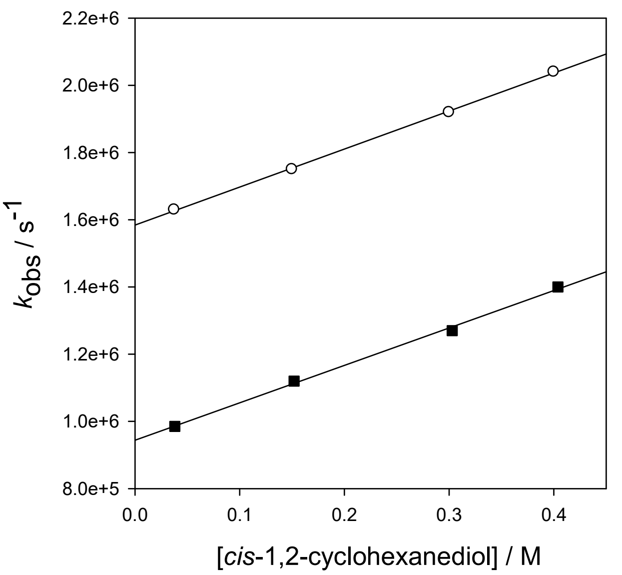

Figure S10. Plot of the observed rate constant (k_{obs}) against [*cis*-1,2-cyclohexanol] for the reactions of CumO$^{\bullet}$ generated by 355 nm LFP of an Ar-saturated MeCN solution containing 1.0 M dicumyl peroxide in the presence of a) $LiClO_4$ 0.5 M (white circles); b) $Mg(ClO_4)_2$ 0.5 M (black squares) measured at T = 25 °C following the decay of CumO$^{\bullet}$ at 490 nm. From the linear regression analysis: a) intercept = 1.58×10^6 s^{-1}, $k_H = 1.13 \times 10^6$ M^{-1} s^{-1}, r^2 = 0.9995; b) intercept = 9.44×10^5 s^{-1}, $k_H = 1.11 \times 10^6$ M^{-1} s^{-1}, r^2 = 0.9978.

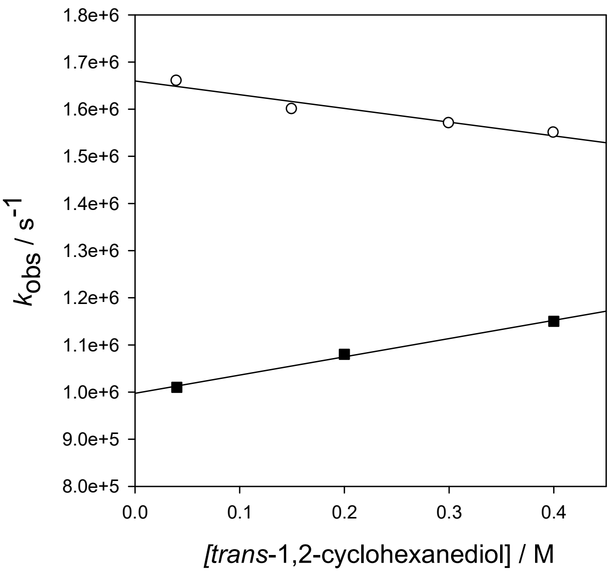

Figure S11. Plot of the observed rate constant (k_{obs}) against [*trans*-1,2-cyclohexanol] for the reactions of CumO$^{•}$ generated by 355 nm LFP of an Ar-saturated MeCN solution containing 1.0 M dicumyl peroxide in the presence of a) $LiClO_4$ 0.5 M (white circles); b) $Mg(ClO_4)_2$ 0.5 M (black squares) measured at T = 25 °C following the decay of CumO$^{•}$ at 490 nm. From the linear regression analysis: a) intercept = 1.70×10^6 s^{-1}; b) intercept = 9.97×10^5 s^{-1}, $k_H = 3.87 \times 10^5$ M^{-1} s^{-1}, $r^2 = 0.9959$.

4) References

S1 M. Salamone, G. Carboni, L. Mangiacapra, M. Bietti, *J. Org. Chem.*, 2015, **80**, 9214-9223.